Molecular Cell, Volume *64*

Supplemental Information

Real-Time Tracking of Parental Histones Reveals Their Contribution to Chromatin Integrity Following DNA Damage

Salomé Adam, Juliette Dabin, Odile Chevallier, Olivier Leroy, Céline Baldeyron, Armelle Corpet, Patrick Lomonte, Olivier Renaud, Geneviève Almouzni, and Sophie E. Polo

Figure S1

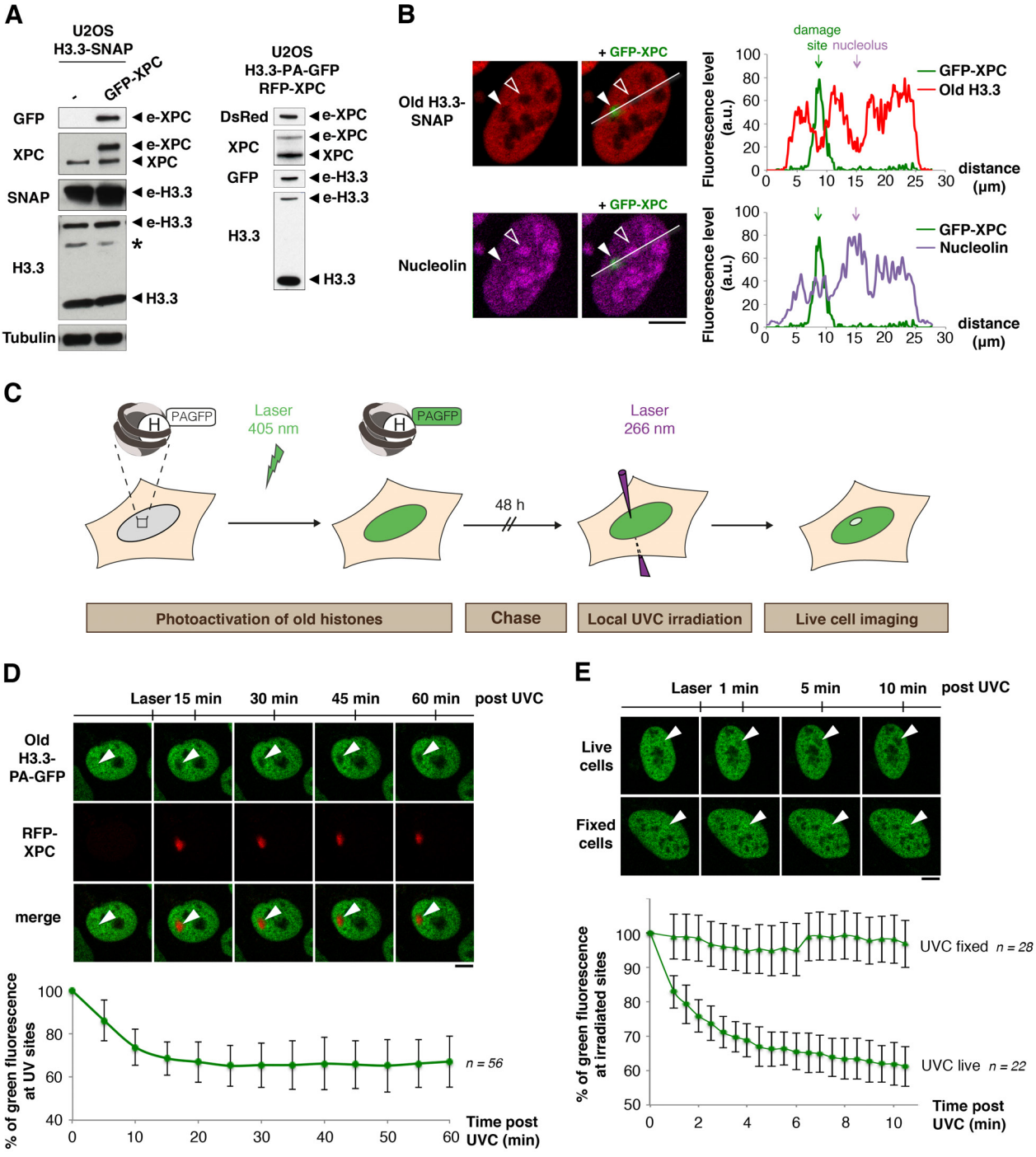
A
U2OS
H3.3-SNAP
-
GFP-XPC
GFP
XPC
SNAP
H3.3
Tubulin
◀ e-XPC
◀ e-XPC
◀ XPC
◀ e-H3.3
◀ e-H3.3
*
◀ H3.3
U2OS
H3.3-PA-GFP
RFP-XPC
DsRed
XPC
GFP
H3.3
◀ e-XPC
◀ e-XPC
◀ XPC
◀ e-H3.3
◀ e-H3.3
◀ H3.3
B
Old H3.3-SNAP
Nucleolin
+ GFP-XPC
+ GFP-XPC
damage site
nucleolus
GFP-XPC
Old H3.3
GFP-XPC
Nucleolin
Fluorescence level (a.u.)
distance (μm)
C
PAGFP
Laser 405 nm
48 h
Laser 266 nm
Photoactivation of old histones
Chase
Local UVC irradiation
Live cell imaging
D
Laser 15 min
30 min
45 min
60 min
post UVC
Old H3.3-PA-GFP
RFP-XPC
merge
% of green fluorescence at UV sites
n = 56
Time post UVC (min)
E
Laser 1 min
5 min
10 min
post UVC
Live cells
Fixed cells
% of green fluorescence at irradiated sites
UVC fixed n = 28
UVC live n = 22
Time post UVC (min)

Figure S1: Rapid decrease in parental H3 histone density in UVC-damaged chromatin regions. Related to Figure 1.

(A) Characterization by western blot of U2OS cell lines stably expressing H3.3-SNAP and GFP-XPC or H3.3-PA-GFP and RFP-XPC. e: epitope tag, *: aspecific band.

(B) Immunostaining for nucleolin in U2OS cells stably expressing H3.3-SNAP and GFP-XPC fixed 15 min after UVC laser micro-irradiation. Parental H3.3-SNAP histones were labeled in red as in Figure 1. Fluorescence profiles along the line crossing the UVC-damaged area (white arrowhead) and a nucleolus (empty arrowhead) are displayed on the graphs.

(C) Scheme of the experimental strategy for tracking parental histone dynamics at DNA damage sites based on photo-activation of PA-GFP-tagged H3.3 histones in the whole nucleus 48 h before UVC laser micro-irradiation and live cell imaging.

(D) Distribution of parental histones H3.3 (green) at the indicated time points after UVC laser micro-irradiation in U2OS cells stably expressing H3.3-PA-GFP and RFP-XPC.

(E) Dynamics of parental histones H3.3 (green) at early time points after local damage induced by UVC laser micro-irradiation as in (D). Paraformaldehyde-fixed cells were used as a control for photo-bleaching of the green fluorescence by the UVC laser. White arrowheads indicate the irradiated areas. The graphs show quantifications of the green fluorescence associated with parental H3.3 in irradiated areas, normalized to the green fluorescence in the same areas before laser micro-irradiation. Error bars represent SD from n cells scored in two independent experiments. Scale bars, 10 μm.

Figure S2

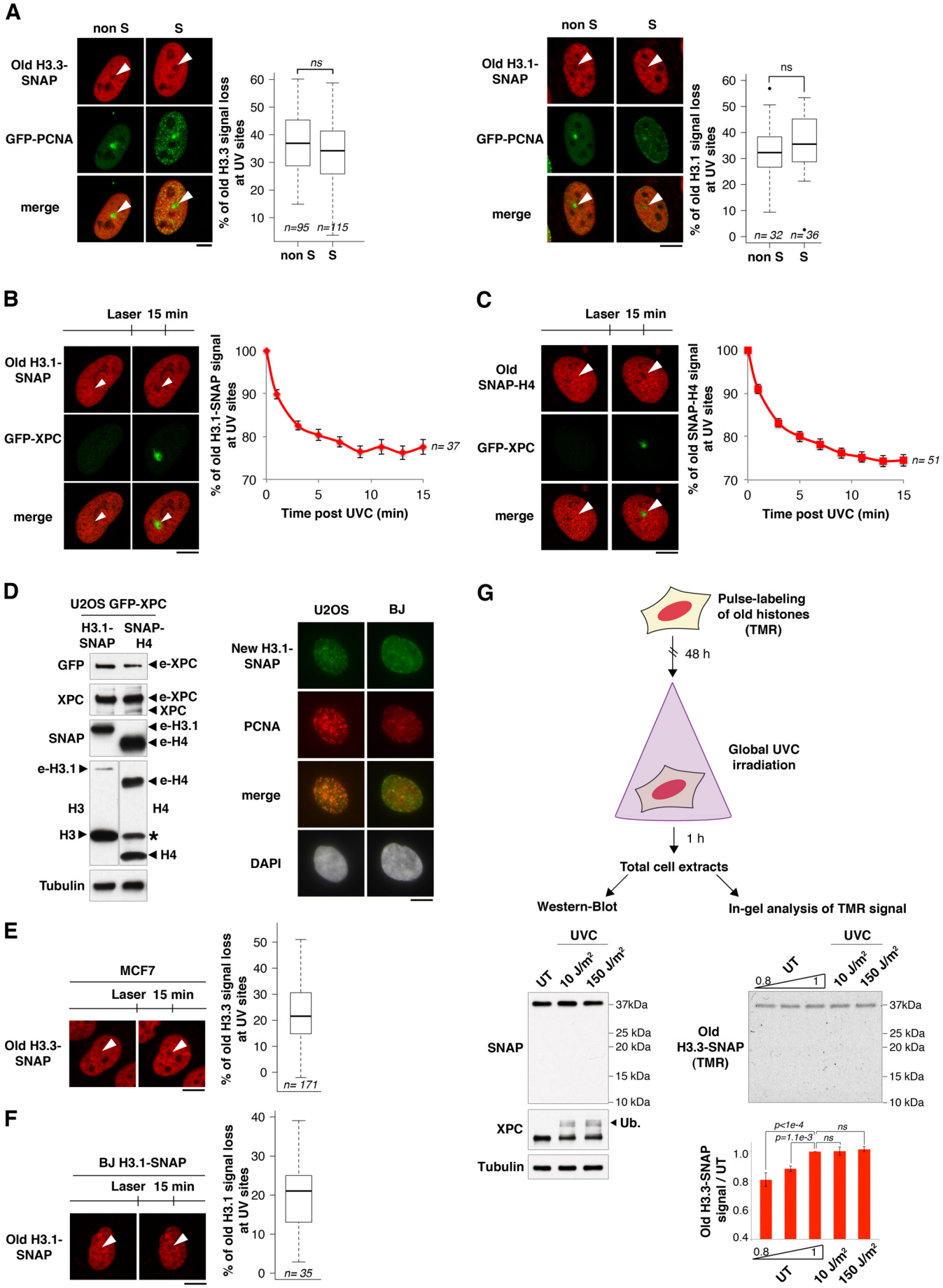
A
non S
S
Old H3.3-SNAP
GFP-PCNA
merge
% of old H3.3 signal loss at UV sites
ns
n=95 n=115
non S S
Old H3.1-SNAP
% of old H3.1 signal loss at UV sites
n= 32 n= 36
B
Laser 15 min
Old H3.1-SNAP
GFP-XPC
% of old H3.1-SNAP signal at UV sites
n= 37
Time post UVC (min)
C
Old SNAP-H4
% of old SNAP-H4 signal at UV sites
n= 51
D
U2OS GFP-XPC
H3.1-SNAP
SNAP-H4
GFP
XPC
SNAP
e-H3.1
H3
H4
Tubulin
e-XPC
e-H4
U2OS
BJ
New H3.1-SNAP
PCNA
merge
DAPI
E
MCF7
Laser 15 min
Old H3.3-SNAP
n= 171
F
BJ H3.1-SNAP
Old H3.1-SNAP
n= 35
G
Pulse-labeling of old histones (TMR)
48 h
Global UVC irradiation
1 h
Total cell extracts
Western-Blot
In-gel analysis of TMR signal
UVC
UT
10 J/m²
150 J/m²
SNAP
XPC
Ub.
Tubulin
37kDa
25 kDa
20 kDa
15 kDa
10 kDa
Old H3.3-SNAP (TMR)
Old H3.3-SNAP signal / UT
p<1e-4
p=1.1e-3
ns

Figure S2: Dynamics of parental H3 and H4 histones in UVC-damaged chromatin. Related to Figures 1 and 2.

(A) Distribution of parental histones H3.3 and H3.1 (red) 15 min after UVC laser micro-irradiation in U2OS cells stably expressing SNAP-tagged H3 variants and transiently transfected with GFP-PCNA. PCNA focal pattern is characteristic of S phase cells.

(B, C) Distribution of parental histones H3.1 (B) and H4 (C) before and 15 min after UVC laser micro-irradiation in U2OS cells stably expressing H3.1-SNAP or SNAP-H4 and GFP-XPC. White arrowheads indicate the irradiated areas. The graphs show quantifications of red fluorescence loss in irradiated areas as a function of time after laser micro-irradiation. Error bars represent SEM from n cells scored in two independent experiments.

(D) Characterization by western blot of U2OS lines stably expressing H3.1-SNAP or SNAP-H4 and GFP-XPC. e: epitope tag, *: aspecific band. We also verified by specific labeling of newly synthesized histones that new H3.1-SNAP displayed characteristic replication-coupled deposition patterns in U2OS and BJ cells. PCNA stains replication foci.

(E, F) Distribution of parental histones H3.3 (E) or H3.1 (F) before and 15 min after UVC laser micro-irradiation in MCF7 cells 96 h post H3.3-SNAP transfection (E) or in BJ cells stably expressing H3.1-SNAP (F). White arrowheads indicate the irradiated areas. The boxplots show quantifications of red fluorescence loss in irradiated areas at 15 min compared to before laser micro-irradiation (data from n cells scored in two independent experiments). Scale bars, 10 μm.

(G) Top: Scheme of the assay for analyzing old H3.3-SNAP protein levels. Global UVC irradiation was carried out at 10 J/m^2 (corresponding to the dose received by the whole nucleus upon laser micro-irradiation) or at 150 J/m^2 (corresponding to 25% of the dose received at the site of laser micro-irradiation for which we expect about 10% reduction in parental histone density at UV sites). Analysis of total H3.3-SNAP levels by western-blot (left) and measurement of old H3.3-SNAP levels by in-gel reading of TMR fluorescence (right) do not reveal any significant decrease in H3.3-SNAP protein levels nor any protein clipping upon UVC irradiation. Different amounts of untreated cell extracts (UT) were loaded to assess that a 10% signal reduction was detectable as shown on the graph quantifying TMR fluorescence intensity associated with H3.3-SNAP bands. XPC ubiquitylation (Ub.) is used as a control for UVC irradiation. ns: non significant.

Figure S3

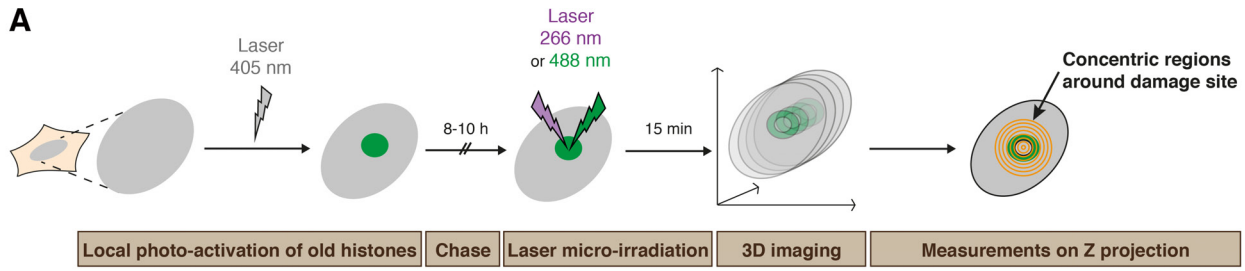
A
Laser
405 nm
Laser
266 nm
or 488 nm
8-10 h
15 min
Concentric regions
around damage site
Local photo-activation of old histones
Chase
Laser micro-irradiation
3D imaging
Measurements on Z projection

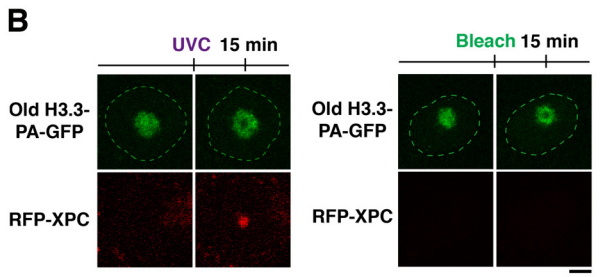
B
UVC 15 min
Bleach 15 min
Old H3.3-
PA-GFP
RFP-XPC

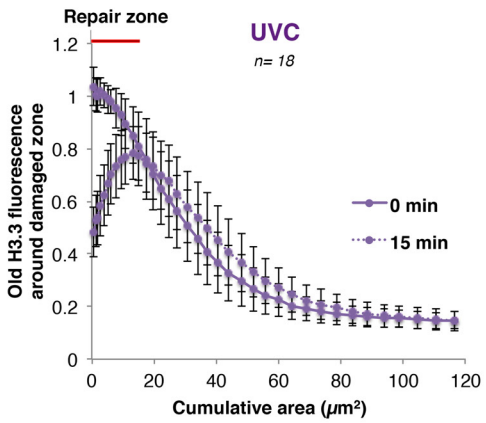
C
Repair zone
UVC
n= 18
Old H3.3 fluorescence
around damaged zone
0 min
15 min
Cumulative area (μm²)

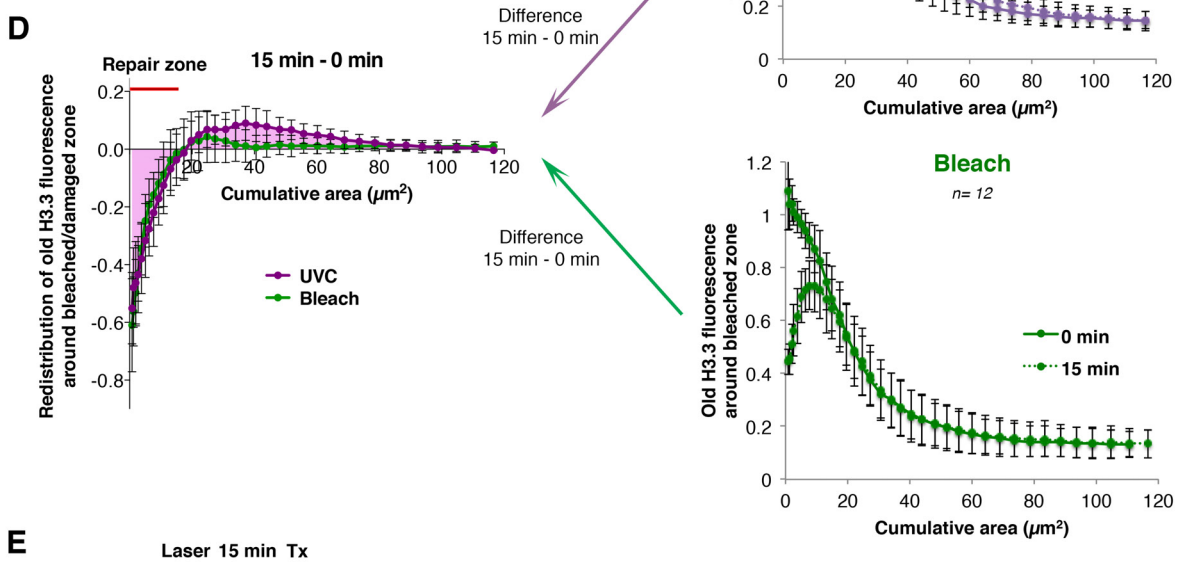
D
Repair zone
15 min - 0 min
Redistribution of old H3.3 fluorescence
around bleached/damaged zone
Cumulative area (μm²)
UVC
Bleach
Difference
15 min - 0 min
Difference
15 min - 0 min
Bleach
n= 12
Old H3.3 fluorescence
around bleached zone
0 min
15 min
Cumulative area (μm²)

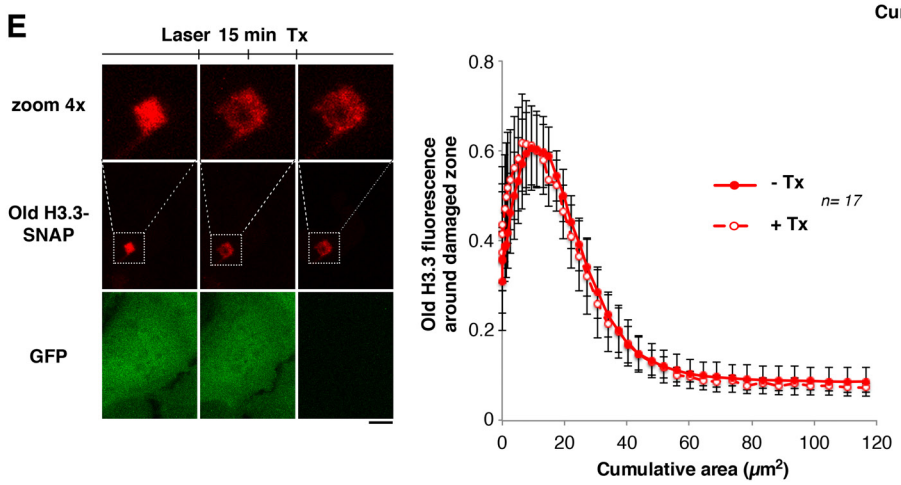
E
Laser 15 min Tx
zoom 4x
Old H3.3-
SNAP
GFP
Old H3.3 fluorescence
around damaged zone
- Tx
+ Tx
n= 17
Cumulative area (μm²)

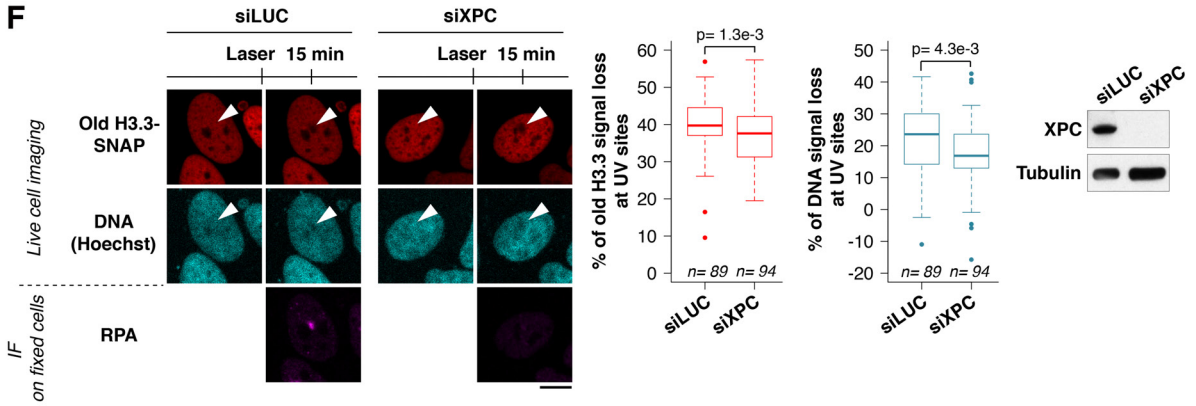
F
siLUC
siXPC
Laser 15 min
Laser 15 min
Live cell imaging
Old H3.3-
SNAP
DNA
(Hoechst)
IF
on fixed cells
RPA
% of old H3.3 signal loss
at UV sites
p= 1.3e-3
n= 89 n= 94
siLUC
siXPC
% of DNA signal loss
at UV sites
p= 4.3e-3
n= 89 n= 94
siLUC
siXPC
siLUC
siXPC
XPC
Tubulin

Figure S3: Conservative redistribution of parental histones to the periphery of UVC-damaged regions. Related to Figures 2 and 3.

(A) Experimental procedure for measuring parental histone loss and redistribution around the UVC damaged area based on photo-activation of a 20 μm^2 patch of pre-existing H3.3-PA-GFP histones in the cell nucleus and micro-irradiation in the center of the fluorescent histone patch with a 266 nm UVC laser (damage induction) or with a 488 nm bleaching laser (control). Fluorescence measurements are performed on 2D projections of 3D acquisitions in concentric regions around the site of laser micro-irradiation.

(B) Fluorescent patches of parental histones H3.3 (green) before and 15 min after local UVC damage (left) or local photo-bleaching (right) in U2OS cells stably expressing H3.3-PA-GFP and RFP-XPC. Green dotted lines delineate the cell nuclei.

(C) Quantification of the green fluorescence associated with parental H3.3-PA-GFP histones in concentric regions around the UVC damage site (purple) or the site of fluorescence bleaching with the 488 nm laser (green) at the indicated time points.

(**D**) Difference in green fluorescence distribution between the two time points obtained by subtracting 0 min from 15 min values quantified in (C). The positive and negative areas under the UVC curve (purple) are equivalent. The position of the repair zone is based on RFP-XPC accumulation at 15 min. Error bars represent SD from n cells scored in two independent experiments.

(E) Fluorescent patches of parental histones H3.3 (red) before and 15 min after UVC laser micro-irradiation, followed by detergent extraction (Tx) in live U2OS cells stably expressing H3.3-SNAP and GFP. GFP solubilization is used as a control for Tx extraction. The graph displays quantification of red fluorescence distribution in concentric regions around the UVC damage site before (-Tx) and after detergent extraction (+Tx). Error bars represent SD from n cells scored in two independent experiments.

(F) Distribution of parental histones H3.3 (red) and DNA (blue, stained with Hoechst) before and 15 min after local UVC irradiation in U2OS cells stably expressing H3.3-SNAP and treated with the indicated siRNAs (siLUC: control). XPC knock-down is verified by western-blot. Upon XPC downregulation, the exposure of single-stranded DNA that normally occurs during the repair process is impaired, as shown by the lack of RPA recruitment, but the reduction in Hoechst staining is still observed. The boxplot shows quantifications of histone (red) and DNA (blue) fluorescence loss in irradiated areas (data from n cells scored in two independent experiments). Scale bars, 10 μm.

Figure S4

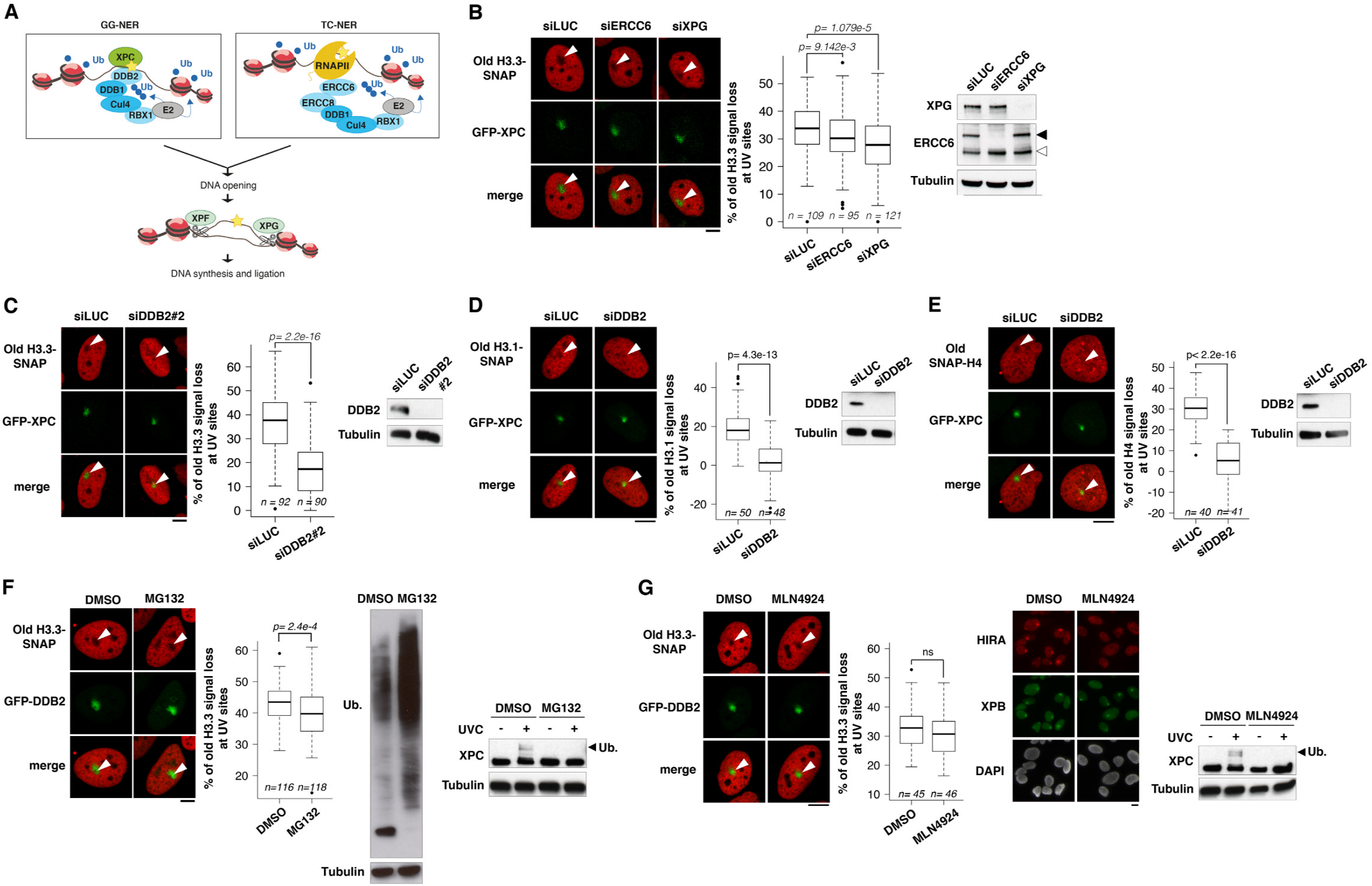
A
GG-NER
TC-NER
XPC
DDB2
DDB1
Cul4
RBX1
E2
Ub
RNAPII
ERCC6
ERCC8
DNA opening
XPF
XPG
DNA synthesis and ligation
B
siLUC
siERCC6
siXPG
Old H3.3-SNAP
GFP-XPC
merge
% of old H3.3 signal loss at UV sites
p= 1.079e-5
p= 9.142e-3
n = 109
n = 95
n = 121
XPG
ERCC6
Tubulin
C
siLUC
siDDB2#2
p= 2.2e-16
n = 92
n = 90
DDB2
D
siDDB2
Old H3.1-SNAP
% of old H3.1 signal loss at UV sites
p= 4.3e-13
n= 50
n= 48
E
Old SNAP-H4
% of old H4 signal loss at UV sites
p< 2.2e-16
n= 40
n= 41
F
DMSO
MG132
GFP-DDB2
% of old H3.3 signal loss at UV sites
p= 2.4e-4
n=116
n=118
Ub.
UVC
XPC
G
MLN4924
ns
n= 45
n= 46
HIRA
XPB
DAPI

Figure S4: Parental histone redistribution is controlled by the repair factor DDB2. Related to Figure 4.
(A) Simplified scheme of the NER pathway showing the different repair factors that were targeted by siRNAs in this study. GG-NER: Global Genome NER, TC-NER: Transcription-Coupled NER.
(B, C) Distribution of parental histones H3.3 (red) 15 min after UVC laser micro-irradiation in U2OS cells stably expressing H3.3-SNAP and GFP-XPC treated with the indicated siRNAs (siLUC: control). siRNA efficiencies were verified by western-blot. The black arrowhead indicates full-length ERCC6 and the empty arrowheads points to a splice variant.
(D, E) Distribution of parental histones H3.1 (D) and H4 (E) 15 min after UVC laser micro-irradiation in U2OS cells stably expressing H3.1-SNAP or SNAP-H4 and GFP-XPC treated with the indicated siRNAs (siLUC: control). siRNA efficiencies were verified by western-blot.
(F, G) Distribution of parental histones H3.3 (red) 15 min after UVC laser micro-irradiation in U2OS cells stably expressing H3.3-SNAP and GFP-DDB2 treated with the proteasome inhibitor MG132 (F) or the neddylation inhibitor MLN4924 (G) (DMSO, vehicle). The efficiency of MG132 treatment was verified by immunoblot against ubiquitin (Ub) showing the accumulation of non-degraded ubiquitylated proteins. Proteasome inhibition by MG132 thus affects *de novo* ubiquitylation by exhausting the pool of free ubiquitin as shown by the lack of XPC ubiquitylation post UVC irradiation. We controlled that the neddylation inhibitor also impairs UVC-induced ubiquitylation of XPC (western-blot) and HIRA accumulation at UVC damage sites (immunofluorescence) by interfering with the activity of the CUL4-DDB1-DDB2 complex. White arrowheads indicate the irradiated areas. Scale bars, 10 μm. The boxplots show quantifications of red fluorescence loss in irradiated areas at 15 min compared to before laser micro-irradiation (data from n cells scored in two independent experiments).

Figure S5

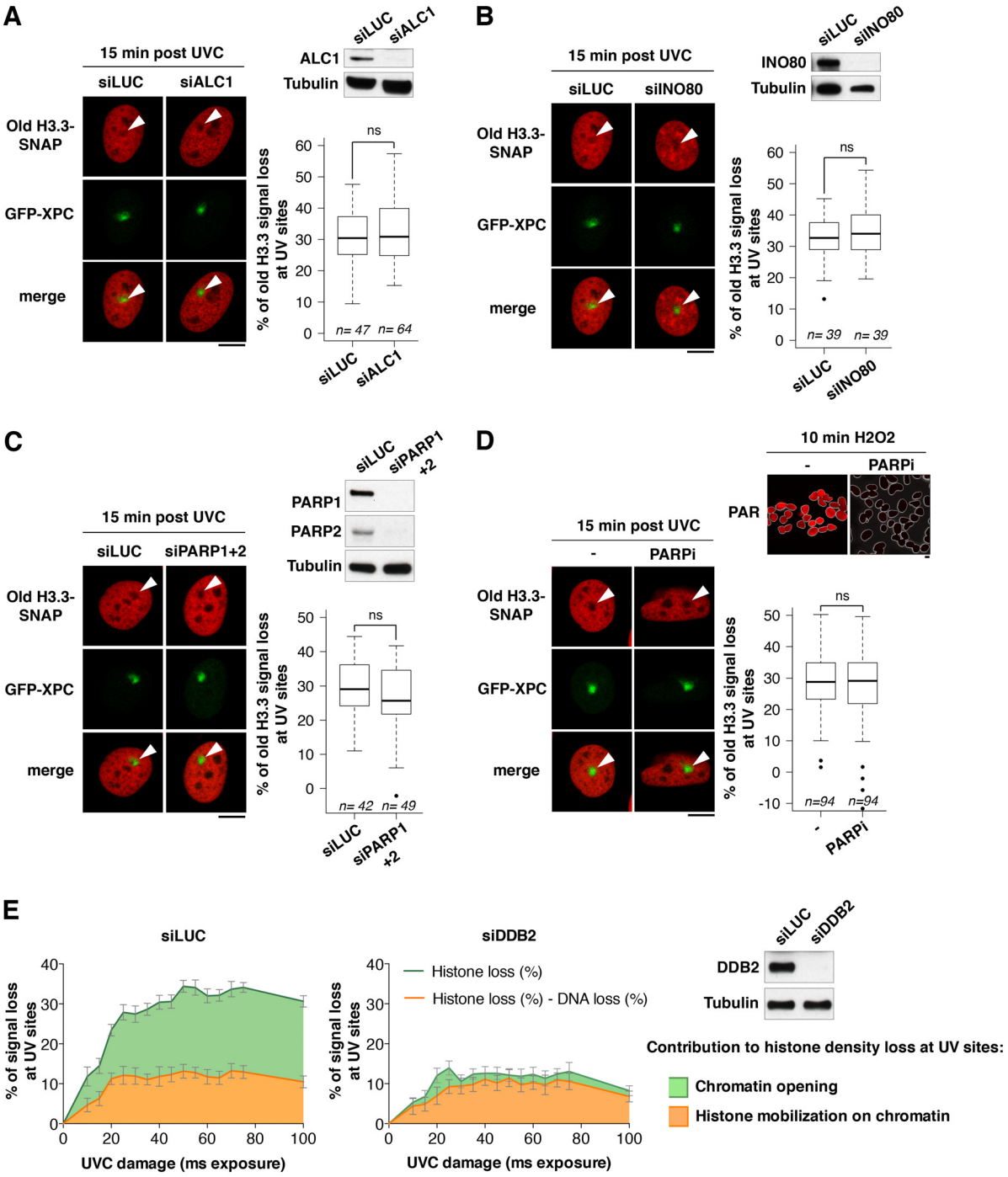
A
15 min post UVC
siLUC
siALC1
Old H3.3-SNAP
GFP-XPC
merge
ALC1
Tubulin
% of old H3.3 signal loss at UV sites
ns
n= 47
n= 64
B
siINO80
INO80
n= 39
n= 39
C
siPARP1+2
PARP1
PARP2
n= 42
n= 49
D
10 min H2O2
-
PARPi
PAR
n=94
n=94
E
siLUC
siDDB2
% of signal loss at UV sites
UVC damage (ms exposure)
Histone loss (%)
Histone loss (%) - DNA loss (%)
DDB2
Contribution to histone density loss at UV sites:
Chromatin opening
Histone mobilization on chromatin

Figure S5: Mechanistic insights into DDB2 function in parental histone dynamics. Related to Figures 3 and 4.

(A-C) Distribution of parental histones H3.3 (red) 15 min after UVC laser micro-irradiation in U2OS cells stably expressing H3.3-SNAP and GFP-XPC treated with the indicated siRNAs (siLUC: control). siRNA efficiencies were verified by western-blot.

(D) Distribution of parental histones H3.3 (red) 15 min after UVC laser micro-irradiation in U2OS cells stably expressing H3.3-SNAP and GFP-XPC treated or not with PARP inhibitor. The efficiency of PARP inhibition was verified by PAR staining after cell treatment with the oxidative agent H_2O_2. White lines delineate nuclear boundaries, based on DAPI staining. White arrowheads indicate the irradiated areas. Scale bars, 10 μm. The boxplots show quantifications of red fluorescence loss in irradiated areas at 15 min compared to before laser micro-irradiation (data from n cells scored in two independent experiments).

(E) Graphs showing chromatin opening (green) and histone mobilization on chromatin (orange) as a function of UVC damage in cells treated with the indicated siRNAs (siLUC: control). Results are based on measurements of parental H3.3 and DNA signal loss in irradiated areas as in Figure 3. DDB2 knock-down is verified by western-blot. Error bars represent SEM from at least 30 cells per time point scored in three independent experiments.

Figure S6

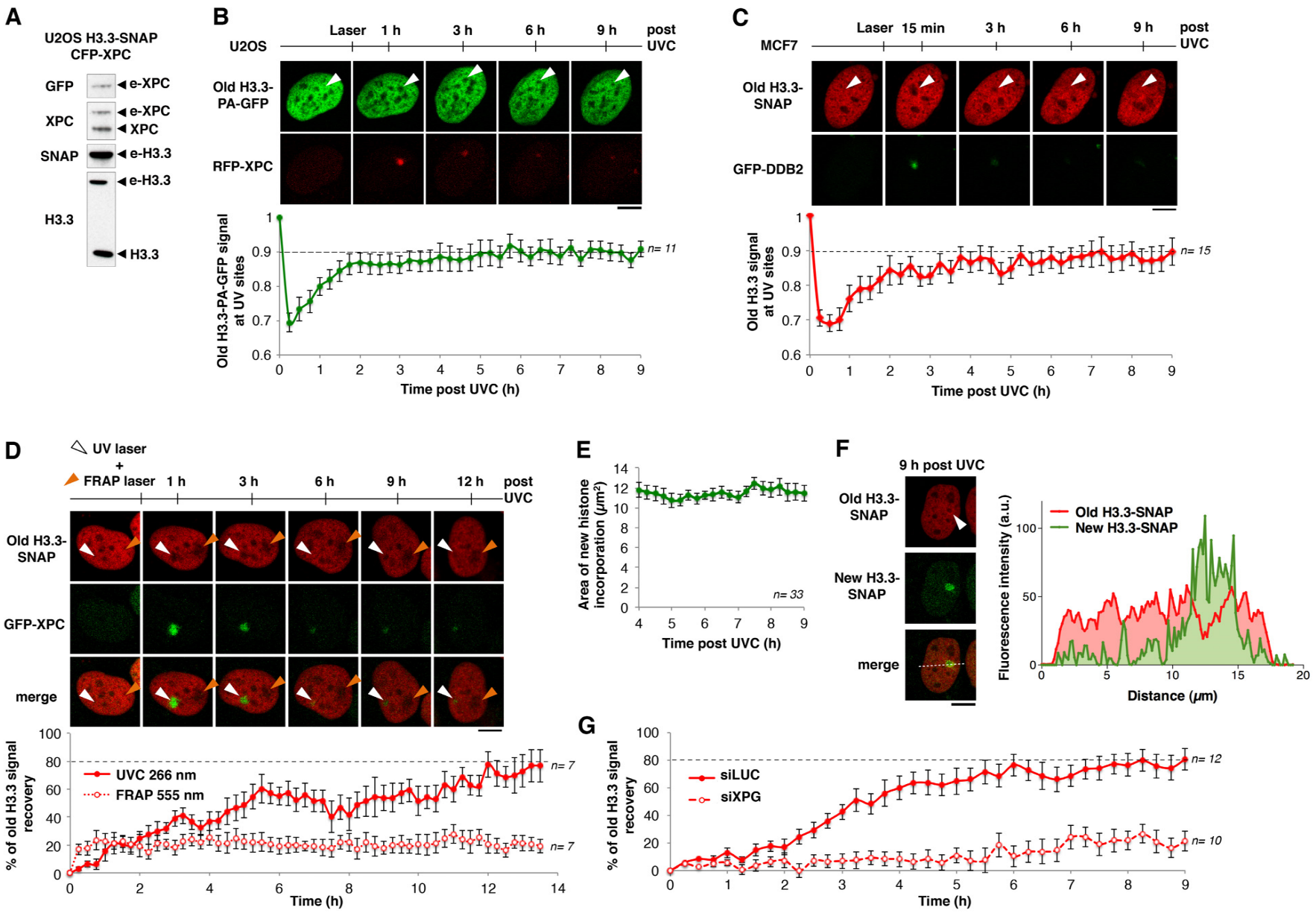
A
U2OS H3.3-SNAP CFP-XPC
GFP
XPC
SNAP
H3.3
e-XPC
e-XPC
XPC
e-H3.3
e-H3.3
H3.3
B
U2OS
Laser 1 h 3 h 6 h 9 h post UVC
Old H3.3-PA-GFP
RFP-XPC
Old H3.3-PA-GFP signal at UV sites
n= 11
Time post UVC (h)
C
MCF7
Laser 15 min 3 h 6 h 9 h post UVC
Old H3.3-SNAP
GFP-DDB2
Old H3.3 signal at UV sites
n= 15
Time post UVC (h)
D
UV laser
+
FRAP laser 1 h 3 h 6 h 9 h 12 h post UVC
Old H3.3-SNAP
GFP-XPC
merge
% of old H3.3 signal recovery
UVC 266 nm
FRAP 555 nm
n= 7
n= 7
Time (h)
E
Area of new histone incorporation (μm²)
n= 33
Time post UVC (h)
F
9 h post UVC
Old H3.3-SNAP
New H3.3-SNAP
merge
Old H3.3-SNAP
New H3.3-SNAP
Fluorescence intensity (a.u.)
Distance (μm)
G
% of old H3.3 signal recovery
siLUC
siXPG
n= 12
n= 10
Time (h)

Figure S6: Recovery of parental histones coupled to repair progression. Related to Figure 6.

(A) Characterization by western blot of the U2OS cell line stably expressing H3.3-SNAP and CFP-XPC. e: epitope tag.

(B) Dynamics of parental histones H3.3 (green) at the indicated time points after local UVC damage (white arrowheads) in U2OS cells stably expressing H3.3-PA-GFP and RFP-XPC. The graph shows quantification of green fluorescence in irradiated areas, normalized to before irradiation.

(C) Dynamics of parental histones H3.3 (red) at the indicated time points after local UVC damage (white arrowheads) in MCF7 cells transiently expressing H3.3-SNAP and GFP-DDB2. The graph shows quantification of red fluorescence in irradiated areas, normalized to before irradiation.

(D) Dynamics of parental histones H3.3 (red) at the indicated points after local damage with the UVC laser (white arrowheads) or after local bleaching of the red fluorescence with a 555 nm laser (orange arrowheads) in U2OS cells stably expressing H3.3-SNAP and GFP-XPC. The graph shows quantification of red fluorescence recovery in illuminated areas. Cells that did not repair efficiently (based on GFP-XPC retention) were excluded from the analysis.

(E) Graph showing the area occupied by newly incorporated H3.3 at the indicated time points after local damage in U2OS cells stably expressing H3.3-SNAP and CFP-XPC. The analysis starts at 4 h post UVC, when new histone deposition reaches a plateau (Figure 6A).

(F) Distribution of parental (red) and newly synthesized H3.3 (green) 9 h after local UVC damage (white arrowhead). Fluorescence profiles along the dotted line crossing the UVC-damaged area are displayed on the graph. a.u.: arbitrary units.

(G) Graph showing the quantification of red fluorescence recovery in irradiated areas in U2OS cells stably expressing H3.3-SNAP and GFP-DDB2 and treated with the indicated siRNAs (data from Figure 5B).

Fluorescence recovery at time t (D and G panels) is calculated as (It-Imin)/(I0-Imin) where 'I' represents the red fluorescence intensity in the illuminated area relative to the entire nucleus, 'I0' is the intensity before irradiation and 'Imin' is the lowest intensity measured. Error bars on the graphs represent SEM from n cells scored in two independent experiments. Scale bars, 10 μm.

SUPPLEMENTAL MOVIES

Movie S1: Parental H3.3 dynamics after local UVC damage (10 min kinetics). Related to Figure 1C.
Dynamics of parental histones H3.3 (red) during the first 10 min after local damage with the UVC laser in U2OS cells stably expressing H3.3-SNAP. 21 images were captured at 30 sec intervals and are displayed at 2 frames/sec. The resulting motion picture is shown with a superimposed white arrowhead pointing to the laser irradiation site.

Movie S2: New H3.3 dynamics after local UVC damage (2 h kinetics). Related to Figure 5A.
Dynamics of newly synthesized histones H3.3 (green) during the first 2 h after local damage with the UVC laser in U2OS cells stably expressing H3.3-SNAP. 25 images were captured at 5 min intervals and are displayed at 2 frames/sec. The resulting motion picture is shown with a superimposed white arrowhead pointing to the laser irradiation site.

Movie S3: Parental H3.3 dynamics after local UVC damage (2 h kinetics). Related to Figure 5A.
Dynamics of parental histones H3.3 (red) during the first 2 h after local damage with the UVC laser in U2OS cells stably expressing H3.3-SNAP. 25 images were captured at 5 min intervals and are displayed at 2 frames/sec. The resulting motion picture is shown with a superimposed white arrowhead pointing to the laser irradiation site.

Movie S4: Parental H3.3 dynamics after local UVC damage (12 h kinetics). Related to Figure 6C.
Dynamics of parental histones H3.3 (red) during the first 12 h after local damage with the UVC laser in U2OS cells stably expressing H3.3-SNAP and GFP-DDB2 treated with siRNA control siLUC. 49 images were captured at 15 min intervals and are displayed at 4 frames/sec. The resulting motion picture (red channel only) is shown with a superimposed white arrowhead pointing to the laser irradiation site.

Movie S5: Parental H3.3 dynamics after local UVC damage (12 h kinetics) in repair-deficient cells. Related to Figure 6C.
Dynamics of parental histones H3.3 (red) during the first 12 h after local damage with the UVC laser in U2OS cells stably expressing H3.3-SNAP and GFP-DDB2 treated with siXPG. 49 images were captured at 15 min intervals and are displayed at 4 frames/sec. The resulting motion picture (red channel only) is shown with a superimposed white arrowhead pointing to the laser irradiation site.

SUPPLEMENTAL EXPERIMENTAL PROCEDURES

Stable cell lines

For stable cell line establishment, U2OS cells were transfected with plasmid DNA 48 h before antibiotic selection of clones. The BJ polyclonal cell line expressing H3.1-SNAP-3xHA was obtained by retroviral transduction. All cell lines were grown at 37°C and 5% CO_2 in Dulbecco's modified Eagle's medium (DMEM, Invitrogen) supplemented with 10% fetal calf serum (EUROBIO), 100 U/mL penicillin and 100 µg/mL streptomycin (Invitrogen) and the appropriate selection antibiotics: Blasticidin (5 µg/ml, Invitrogen), G418 (100 µg/mL, Invitrogen), Hygromycin (200 µg/mL, Euromedex).

Cell line (reference)	Selection antibiotics
BJ H3.1-SNAP-3xHA	Blasticidin
MCF7	None
U2OS H3.3-SNAP (Dunleavy et al., 2011)	G418
U2OS H3.3-SNAP GFP	G418
U2OS H3.3-SNAP GFP-XPC	G418 + Hygromycin
U2OS H3.3-SNAP CFP-XPC	G418 + Hygromycin
U2OS H3.3-SNAP GFP-DDB2	G418 + Hygromycin
U2OS H3.1-SNAP GFP-XPC (U2OS H3.1 SNAP from Dunleavy et al., 2011)	G418 + Hygromycin
U2OS SNAP-H4 GFP-XPC	G418 + Hygromycin
U2OS H3.3-PA-GFP RFP-XPC	G418 + Hygromycin
U2OS LacO H3.3-SNAP (U2OS LacO with 256 tandem LacO repeats from Beuzer et al., 2014; Soutoglou et al., 2007)	G418

Plasmids.

All the coding sequences for histone variants and repair factors are of human origin except lacR-fused DDB2, which is murine. All constructs were verified by direct sequencing and/or restriction digests. Cloning details and primer sequences (Sigma-Aldrich) are available upon request.

Plasmid	Construct details
H3.3-SNAP	*H3F3B* coding sequence cloned into pSNAPm (New England Biolabs) (Dunleavy et al., 2011)
H3.1-SNAP	*HIST1H3C* coding sequence cloned into pSNAPm (New England Biolabs) (Dunleavy et al., 2011)
H3.1-SNAP-3xHA	pBABE-Blasti H3.1-SNAP-3xHA plasmid described in (Ray-Gallet et al., 2011)
H3.3-PA-GFP	*H3F3B* coding sequence in frame with PA-GFP in PA-GFP-N1 (Patterson and Lippincott-Schwartz, 2004) subcloned into pSNAPm replacing the SNAP tag sequence
SNAP-H4	*HIST1H4J* coding sequence cloned into pSNAPm (New England Biolabs)
GFP	pEGFP-C1 (Clontech)
GFP-PCNA	(Leonhardt et al., 2000)
GFP-XPC	Flag-GFP-XPC in pIREShyg (Clontech) (Nishi et al., 2009)
RFP-XPC	RFP from mRFP-C1 (Campbell et al., 2002) subcloned into CFP-XPC plasmid, replacing CFP
CFP-XPC	CFP-XPC (Montpellier Genomic Collections) subcloned into pBabe Hygro (Cell Biolabs)
GFP-DDB2	*DDB2* coding sequence (Montpellier Genomic Collections) subcloned into GFP-XPC plasmid, replacing XPC
mCherry-lacR	mCherry-lacR-NLS (Soutoglou and Misteli, 2008)
mCherry-lacR-DDB2	DDB2 in mCherry-lacR (Luijsterburg et al., 2012)

Drug treatments

DNA was stained by incubating live cells with Hoechst 33258 (10 µg/mL final concentration, Sigma-Aldrich) for 30 min at 37°C before the analysis. Detergent extraction on live cells was performed with 0.5% Triton-X-100 in CSK buffer (Cytoskeletal buffer: 10 mM PIPES pH 7.0, 100 mM NaCl, 300 mM sucrose, 3 mM $MgCl_2$). The PARP inhibitor KU-58948 (gift from S. Jackson laboratory) was added to the culture medium at 10 µM final

concentration 1 h before irradiation. The neddylation inhibitor MLN4924 (Merck Millipore) was added to the culture medium at 2 μM final concentration 30 min before irradiation. Proteasome inhibition was performed by adding MG132 to the culture medium for 2 h at 37°C before the analysis (10 μM final concentration, Enzo Life Science). Treatment of cells with H_2O_2 (1 mM final, VWR Chemicals) was for 10 min on ice. LacR-DDB2 release from the Lac operator was achieved by adding IPTG (isopropyl β-D-1-thiogalactopyranoside, 10 mM final concentration, Euromedex) to the culture medium in which the usual serum is replaced by Tetracycline-free fetal calf serum (Biowest). For long-term experiments on live cells, Hepes buffer was added to the culture medium (25 mM final concentration, Sigma-Aldrich).

siRNA sequences.
All siRNAs were purchased from Eurofins MWG Operon. The final concentration of each siRNA in the culture medium was 50 nM. Cells were analyzed and/or harvested 72 h post-transfection. When performing over-night experiments with mixed cell populations treated with different siRNAs, one of the two cell populations was stained with Cell Tracker Deep Red (Life Technologies) following manufacturer's instructions.

Designation	Target sequence
siALC1	5' UCUACUCCCUCCUCAGUUU 3'
siCUL4A	5'GAAUCCUACUGCUGAUCGA3'
siDDB1	5'GCAAGGACCUGCUGUUUAU3'
siDDB2	5'UCACUGGGCUGAAGUUUAA3',
siDDB2#2	5'UCAGUUCGCUUAAUGAAUU3'
siERCC6	5'GAAGAGUUGUCAGUGAUUA3'
siH3.3	1:1 combination of siH3.3A: 5'CUACAAAAGCCGCUCGCAA3' and siH3.3B: 5'GCUAAGAGAGUCACCAUCAU3'
siHIRA	5'GGAGAUGACAAACUGAUUA3'
siINO80	5' GGAGUUAUUUGAACGGCAA 3'
siLUC (Luciferase)	5'CGUACGCGGAAUACUUCGA3'
siPARP1	5' GGGCAAGCACAGUGUCAAA 3'
siPARP2	5' AGAUGAUGCCCAGAGGAAC 3'
siXPC	5' GCAAAUGGCUUCUAUCGAA 3'
siXPG	5'GAAAGAAGAUGCUAAACGU3'

SNAP labeling and photo-activation of histones
Pre-existing SNAP-tagged histones were labeled by incubating cells with 2 μM red-fluorescent SNAP reagent (SNAP-cell TMR star, New England Biolabs) or 4 μM green-fluorescent SNAP reagent (SNAP-cell Oregon Green, New England Biolabs) for 20 min (pulse), followed by a 30 min-incubation in fresh medium. Cells were subject to laser micro-irradiation and imaging 48 h after the pulse.
For specific labeling of newly-synthesized histones, pre-existing SNAP-tagged histones were first quenched by incubating cells with 10 μM SNAP-cell Block (New England Biolabs) for 30 min followed by a 30 min-wash in fresh medium and a 2 h-chase. The SNAP-tagged histones neo-synthesized during the chase were then pulse-labeled as described above. Cells were subject to local UVC irradiation immediately afterwards.
Laser settings for photo-activation were: maximum power, 5 iterations, 6.30 μsec/pixel scan speed. We photo-activated either total nuclei 48 h prior to local UVC irradiation or a nuclear region of 50 μm^2 8 to 10 h before local UVC irradiation to minimize the distortion of the photo-activated area due to cell movement and cell division.

UVC laser micro-irradiation
For laser-induction of UVC damage, cells were grown on quartz coverslips (SPI supplies) and irradiated for 50 ms unless stated otherwise using a 2 mW pulsed diode-pumped solid-state laser emitting at 266 nm (repetition rate up to 10 kHz, Rapp OptoElectronics, Hamburg GmbH) on a Zeiss LSM 700 confocal microscope adapted for UVC transmission with all-quartz optics. The laser was attenuated using a neutral density filter OD1 (10%T) and focused through a quartz 40x/0.6 Ultrafluar glycerol objective (Carl Zeiss) to yield a spot size of 2 μm in diameter, damaging ca. 2% of the nuclear volume. In these conditions, UVC laser damage did not cause major cytotoxicity as the mortality rate over a 14 h live cell imaging experiment after laser damage was only around 10% and damaged cells did repair and went through mitosis. The UVC dose delivered at the site of laser micro-irradiation was estimated at 600 J/m^2 - corresponding to ca. 1 UV lesion per nucleosome - by comparing the intensity of GFP-XPC recruitment upon local UVC irradiation in the same nucleus with the 266 nm laser and with a 254 nm lamp through a micropore filter (Millipore). The dose delivered by the UVC lamp was measured with a VLX-3W dosimeter (Vilbert-Lourmat).

Local UVC irradiation through micropore filters
Cells grown on glass coverslips (VWR) were covered with a polycarbonate filter (5 μm pore size, Millipore) and irradiated with 150 J/m^2 UVC (254 nm) using a low-pressure mercury lamp. Conditions were set using a VLX-3W dosimeter (Vilbert-Lourmat).

FRAP (Fluorescence Recovery After Photo-bleaching)
Bleaching of the red fluorescence was performed on a Zeiss LSM700 confocal microscope with a 10 mW 555 nm laser (laser settings: maximum power, 4 iterations, 1.58 μ sec/pixel scan speed). Bleaching of the green fluorescence was performed using a 10 mW 488 nm laser (laser settings: maximum power, 15 iterations, 6.30 μ sec/pixel scan speed). In both cases, the laser was focused through a LD LCI Plan-Apochromat 25x/0.8 multi-immersion objective, the bleached area was 10 μm^2 and bleaching conditions were set to reach a local loss of fluorescence similar to the loss of signal observed 15 min after UVC laser damage. For bleaching of the red fluorescence in the entire nucleus to leave a small fluorescent patch of 20-25 μm^2, the laser settings were changed to 10 iterations and 12.61 μ sec/pixel scan speed.

Image acquisition and analysis
Live cell imaging of LacR-DDB2 dynamics was performed on a Zeiss LSM710 confocal microscope using a Plan-Apochromat 63x/1.4 oil objective. Live cell imaging coupled to local UVC irradiation was performed using a LD LCI Plan-Apochromat 25x/0.8 multi-immersion objective on a Zeiss LSM700 confocal microscope equipped with a UVC laser to inflict damage and adapted for UVC transmission with all quartz optics. Cells were kept at 37°C during acquisition using a microscope incubator system (PeCon). The fluorescence-based autofocus mode was activated in order to acquire images from the best focal plane. Image J software (U. S. National Institutes of Health, Bethesda, Maryland, USA, http://imagej.nih.gov/ij/) was used for image analysis. To correct for overall bleaching of the signal due to repetitive imaging, fluorescence intensities were normalized against intensities measured in an undamaged nucleus in the same field. The extent of fluorescence loss at irradiated sites was determined by dividing the fluorescence intensity in the illuminated area by the fluorescence intensity of the entire nucleus, after background subtraction. The illuminated area was defined at 10-15 min post irradiation, based on fluorescently-labeled XPC or based on fluorescence loss, and was kept the same for all time points. Fluorescence recovery in the illuminated region was calculated relative to before illumination and starting from the time point with minimum intensity. The areas of low parental histone density and of new histone incorporation were measured using the inbuilt Moments threshold (on inverted images for parental histone signal). The GFP-XPC and CPD areas (damaged chromatin) were measured using the inbuilt Yen threshold (set from 20 to 225 for CPD measurement). In this analysis, we verified that there was no significant difference in CPD signals (Integrated Density) between 0 and 15 min post UVC, which is expected given the long time scale of CPD repair. 2D projections of 3D images from z-stack acquisitions (Figure 2 and S2) were obtained by maximum intensity z-projection (note that comparable results were obtained when running image analyses on 3D acquisitions and on maximum intensity projections using Imaris software). On these projections, fluorescence intensity was measured in the micro-irradiated zone, in the entire nucleus and in concentric circular regions spaced by 1 pixel and centered on the laser micro-irradiation site using a custom Image J macro. In this analysis, we systematically verified that the largest circle was within the boundaries of the cell nucleus.

Cell extracts and western blot
Total extracts were obtained by scraping cells in Laemmli buffer (50 mM Tris HCl pH 6.8, 1.6% SDS (Sodium Dodecyl Sulfate), 8% glycerol, 4% β-mercaptoethanol, 0.0025% bromophenol blue) followed by 5 min denaturation at 95°C. For western blot analysis, extracts were run on 4%–20% Mini-PROTEAN TGX gels (Bio-Rad) in running buffer (200 mM glycine, 25 mM Tris, 0.1% SDS) and transferred onto nitrocellulose membranes (Protran) with a Trans-Blot SD semidry transfer cell (Bio-Rad). Total proteins were revealed by reversible protein stain (Pierce). Proteins of interest were probed using the appropriate primary and HRP (Horse Radish Peroxidase)-conjugated secondary antibodies (Jackson Immunoresearch), detected using Super-Signal West Pico or Femto chemiluminescence substrates (Pierce).

Immunofluorescence
Cells grown on glass coverslips (VWR) were fixed directly with 2% paraformaldehyde and permeabilized with 0.2% Triton X-100 in PBS or pre-extracted before fixation with 0.5% Triton-X-100 in CSK buffer (Cytoskeletal buffer: 10 mM PIPES pH 7.0, 100 mM NaCl, 300 mM sucrose, 3 mM $MgCl_2$) for 5 min. Methanol fixation was used for PCNA staining. For CPD staining, DNA was denatured with 0.5 M NaOH for 5 min. Samples were blocked in 5% BSA (Bovine Serum Albumin, Sigma-Aldrich) in PBS supplemented with 0.1% Tween before incubation with primary antibodies and secondary antibodies conjugated to Alexa-Fluor dyes (Invitrogen). Coverslips were mounted in Vectashield medium with DAPI (Vector laboratories).

Antibodies

	Antibody	Species	Dilution	Application	Supplier (reference)
Primary	**ALC1**	Mouse	1:1000	WB	Abcam (ab51324)
	CPD	Mouse	1:1000	IF	Kamiya Biomedical Company (MC-062)
	CUL4A	Rabbit	1:2000	WB	Bethyl Laboratories (A300-739A)
	DDB1	Rabbit	1:2000	WB	Abcam (ab21080)
	DDB2	Mouse	1:200	WB	Abcam (ab51017)
	DsRed	Rabbit	1:1000	WB	Clontech (632496)
	ERCC6	Rabbit	1:500	WB	Santa Cruz Biotechnology (sc-25370)
	GFP	Mouse	1:1000	WB	Roche Applied Science (11814460001)
	H3	Rabbit	1:500	WB	Sigma Aldrich (H9289)
	H3.3	Mouse	1:200	WB	Abnova (H00003021-M01)
	H4	Rabbit	1:1000	WB	Cell Signaling Technology (13919)
	HIRA	Mouse	1:200/1:100	WB/IF	Active Motif (39557)
	INO80	Rabbit	1:1000	WB	Euromedex (A303-371A)
	Nucleolin	Rabbit	1:1000	IF	Santa Cruz Biotechnology (sc-13057)
	PAR	Rabbit	1:100	IF	Trevigen (4336-BPC-100)
	PARP1	Rabbit	1:1000	WB	Cell Signaling Technology (9542)
	PARP2	Rabbit	1:1000	WB	Enzo Life Sciences (ALX-210-303)
	PCNA	Mouse	1:1000	IF	DAKO (M0879)
	RPA	Mouse	1:500	IF	Abcam (ab2175)
	SNAP	Rabbit	1:1000	WB	Pierce Antibodies (CAB4255)
	Tubulin	Mouse	1:10 000	WB	Sigma-Aldrich (T9026)
	XPB	Rabbit	1:400	IF	Santa Cruz Biotechnology (sc-293)
	XPC	Mouse	1:500	WB	Genetex (GTX70294)
	XPG	Rabbit	1:500	WB	Bethyl Laboratories (A301-484A)
Secondary	**Anti-Mouse HRP**	Goat	1:10 000	WB	Jackson Immunoresearch (115-035-068)
	Anti-Rabbit HRP	Donkey	1:10 000	WB	Jackson Immunoresearch (711-035-152)
	Anti-Rabbit Alexa Fluor 680	Goat	1:1000	IF	Invitrogen (A21109)
	Anti-Mouse Alexa Fluor 647	Goat	1:1000	IF	Invitrogen (A21236)
	Anti-Mouse Alexa Fluor 594	Goat	1:1000	IF	Invitrogen (A11032)
	Anti-Rabbit Alexa Fluor 594	Goat	1:1000	IF	Invitrogen (A11037)
	Anti-Rabbit Alexa Fluor 488	Goat	1:1000	IF	Invitrogen (A11034)

Quantification of parental histone protein amounts following global UVC irradiation

Parental H3.3-SNAP histones were labeled by incubating U2OS H3.3-SNAP cells with 2 µM SNAP-cell TMR star (New England Biolabs) for 20 min. Cells were globally irradiated 48 h later with UVC (254 nm) at the indicated doses using a low-pressure mercury lamp. Conditions were set using a VLX-3W dosimeter (Vilbert-Lourmat). One hour after irradiation, cells were harvested in Laemmli buffer. Total protein concentration in each sample was measured on a DS-11 FX+ spectrophotometer (DeNovix). Equal protein amounts were loaded on 4%–20% Mini-PROTEAN TGX gels (Bio-Rad) for electrophoresis followed by western-blot or in-gel

fluorescence analysis of TMR-star fluorescence with a Typhoon FLA-7000 (GE Healthcare-Life Sciences). The intensities of fluorescent bands corresponding to TMR star-labeled parental H3.3-SNAP were quantified using ImageJ software.

Quantitative RT-PCR

RNA extracted from cells with Trizol (Invitrogen) and precipitated in isopropanol was subject to DNA digestion with Turbo DNA-free (Life technologies) and reverse transcribed with Superscript III RT using random primers (Life technologies). Quantitative PCR reactions were carried out with the indicated primer pairs and the Power SYBR® Green PCR Master Mix (Life Technologies) and read in 96-well plates (MicroAmp® Fast Optical, Life Technologies) using a ABI 7500 Fast detection system (Life Technologies). Results were normalized to the amount of the GAPDH gene product.

PCR primers

Designation	Sequence	Final concentration	Supplier
H3F3A_F	$^{5'}$GATGGCAACTAAATGGTGTTTG$^{3'}$	500 nM	Eurofins MWG Operon
H3F3A_R	$^{5'}$CAGGAACAGCACAGAAGACAG$^{3'}$		
H3F3B_F	$^{5'}$CAACCCAGAAGGCGAAGATA$^{3'}$		
H3F3B_R	$^{5'}$TTTCTCCTTTGCCTCTGCTC$^{3'}$		
GAPDH_F	$^{5'}$CAAGGCTGTGGGCAAGGT$^{3'}$		
GAPDH_R	$^{5'}$GGAAGGCCATGCCAGTGA$^{3'}$		

F : forward ; R : reverse.

SUPPLEMENTAL REFERENCES

Beuzer, P., Quivy, J.-P., and Almouzni, G. (2014). Establishment of a replication fork barrier following induction of DNA binding in mammalian cells. Cell Cycle *13*, 1607–1616.

Campbell, R.E., Tour, O., Palmer, A.E., Steinbach, P.A., Baird, G.S., Zacharias, D.A., and Tsien, R.Y. (2002). A monomeric red fluorescent protein. Proc. Natl. Acad. Sci. U.S.a. *99*, 7877–7882.

Dunleavy, E.M., Almouzni, G., and Karpen, G.H. (2011). H3.3 is deposited at centromeres in S phase as a placeholder for newly assembled CENP-A in G1 phase. Nucleus *2*, 146–157.

Leonhardt, H., Rahn, H.P., Weinzierl, P., Sporbert, A., Cremer, T., Zink, D., and Cardoso, M.C. (2000). Dynamics of DNA replication factories in living cells. J. Cell Biol. *149*, 271–280.

Luijsterburg, M.S., Lindh, M., Acs, K., Vrouwe, M.G., Pines, A., van Attikum, H., Mullenders, L.H., and Dantuma, N.P. (2012). DDB2 promotes chromatin decondensation at UV-induced DNA damage. J. Cell Biol. *197*, 267–281.

Nishi, R., Alekseev, S., Dinant, C., Hoogstraten, D., Houtsmuller, A.B., Hoeijmakers, J.H.J., Vermeulen, W., Hanaoka, F., and Sugasawa, K. (2009). UV-DDB-dependent regulation of nucleotide excision repair kinetics in living cells. DNA Repair (Amst.) *8*, 767–776.

Patterson, G.H., and Lippincott-Schwartz, J. (2004). Selective photolabeling of proteins using photoactivatable GFP. Methods (San Diego, Calif) *32*, 445–450.

Ray-Gallet, D., Woolfe, A., Vassias, I., Pellentz, C., Lacoste, N., Puri, A., Schultz, D.C., Pchelintsev, N.A., Adams, P.D., Jansen, L.E.T., et al. (2011). Dynamics of histone H3 deposition in vivo reveal a nucleosome gap-filling mechanism for H3.3 to maintain chromatin integrity. Mol. Cell *44*, 928–941.

Soutoglou, E., and Misteli, T. (2008). Activation of the cellular DNA damage response in the absence of DNA lesions. Science *320*, 1507–1510.

Soutoglou, E., Dorn, J.F., Sengupta, K., Jasin, M., Nussenzweig, A., Ried, T., Danuser, G., and Misteli, T. (2007). Positional stability of single double-strand breaks in mammalian cells. Nat. Cell Biol. *9*, 675–682.